Bulletin of Electrical Engineering and Informatics
Vol. 14, No. 6, December 2025, pp. 4368~4376
ISSN: 2302-9285, DOI: 10.11591/eei.v14i6.10594

Path planning and obstacle avoidance for UAVs using Theta* and modulated velocity obstacle avoidance with 2D LiDAR

Hoang Thuan Tran, Dong LT. Tran, Chi Thanh Vo
Institute of Aerospace Engineering and Technology, Duy Tan University, Da Nang, Vietnam

Article Info

Article history:

Received Apr 29, 2025
Revised Oct 3, 2025
Accepted Oct 14, 2025

Keywords:

Dynamic window approach
LiDAR
Modulated velocity obstacle avoidance
Theta*
Unmanned aerial vehicle

ABSTRACT

This paper proposes a novel framework for autonomous unmanned aerial vehicle (UAV) navigation in complex environments, seamlessly integrating Theta* for global path planning with a simplified modulated velocity obstacle avoidance (MVOA) algorithm for local obstacle avoidance. Theta* generates optimal, smooth paths, while MVOA processes 2D LiDAR data as a single obstacle block to compute modulated velocities, enabling efficient avoidance of static and dynamic obstacles with minimal computational overhead. Compared to MVOA-only navigation, the integration of Theta* and MVOA produced shorter trajectories and faster mission completion with smoother velocity adjustments, demonstrating clear improvements in efficiency and stability. Simulation results show the framework maintains a 0.6 m safety distance and operates at 10 Hz, underscoring its robustness and reliability. The resulting control velocity is transmitted to an ArduPilot-based flight controller via MAVLink, ensuring precise, real-time execution. The current implementation focuses on 2D navigation in a planar environment as a foundation for future 3D expansion, with all results obtained through high-fidelity simulation. Building on these findings, the framework shows strong potential for real-time applications such as swarm UAV coordination, terrain surveying, and indoor navigation, offering a scalable solution for autonomous systems in dynamic settings.

Corresponding Author:

Chi Thanh Vo
Institute of Aerospace Engineering and Technology, Duy Tan University
Da Nang, 550000, Vietnam
Email: vochithanh1@dtu.edu.vn

1. INTRODUCTION

Unmanned aerial vehicles (UAVs) are increasingly applied in terrain surveying [1], precision agriculture [2], disaster response [3], and swarm coordination [4]. These missions demand robust autonomous navigation in cluttered and dynamic environments such as narrow passages or urban areas [5], [6]. Effective navigation requires the integration of global path planning for optimal routing and local obstacle avoidance for real-time safety [7], yet achieving this balance with lightweight computation remains challenging [8], [9]. No single approach fully addresses the range of UAV mission requirements [10], [11].

Classical methods show clear trade-offs. The dynamic window approach (DWA) [12] ensures effective local avoidance but is computationally expensive, even with recent dual-filter safety extensions [13]. Vector field histogram (VFH) [14] enables fast histogram-based avoidance but suffers from local minima, only partially mitigated by fisheye-based object detection [15]. Global planners such as A* [16] provide reliable paths but generate grid-aligned trajectories unsuited to UAV maneuverability.

To overcome these limitations, we propose a hybrid framework integrating Theta* [17], [18] and a modulated velocity obstacle avoidance (MVOA) algorithm [19], [20]. Theta*, an any-angle extension of A*,

reduces path length and improves smoothness compared to grid-constrained methods, with recent risk-aware and learning-based adaptations further enhancing UAV efficiency [21], [22]. MVOA complements this by processing raw 2D LiDAR scans into a unified obstacle block, avoiding clustering or predictive tracking while ensuring safe, real-time avoidance with minimal overhead [23].

Recent studies highlight the need to fuse global and local strategies [24], teach-repeat-replan [25], velocity obstacles with onboard perception [26], or hybrid DWA–potential field [27]. While these approaches improve reactivity, they often require costly computations [28] or sacrifice global efficiency [29]–[31]. In contrast, our Theta*+MVOA framework introduces three key novelties: i) a bidirectional loop where MVOA not only follows Theta* waypoints but also triggers replanning if blocked, ii) a lightweight velocity modulation using adaptive weights and predictive safety checks, and iii) direct use of raw LiDAR scans without dense mapping.

Finally, a crucial step in UAV autonomy is translating paths and velocities into flight commands. Using ArduPilot and the MAVLink protocol provides a robust control backbone, yet their integration with advanced planners in ROS Noetic simulation environments (Gazebo, RViz) remains underexplored. To address this, we present a cohesive framework combining enhanced Theta* and simplified MVOA, validated in a 10 m×10 m Gazebo environment with static and dynamic obstacles.

The remainder of this paper is organized as follows: section 2 presents the methodology; section 3 presents the results and discussion; and section 5 concludes the paper and provides future directions.

2. METHOD

2.1. System overview

The proposed framework (Figure 1) enables autonomous UAV navigation in complex and dynamic environments by integrating global path planning, local obstacle avoidance, and real-time flight control.

- Global planner: Theta* [17], [18] generates smooth waypoints wpwpwp on a 1 m×1 m occupancy grid, ensuring efficient, low-cost trajectories.
- Local planner: MVOA [20] processes 2D LiDAR scans to compute a modulated velocity v_{mo}, enabling safe obstacle avoidance while following Theta* waypoints.
- Control interface: v_{mo} is converted into MAVLink commands for ArduPilot, which adjusts UAV speed and orientation in real time for robust indoor/outdoor flight.

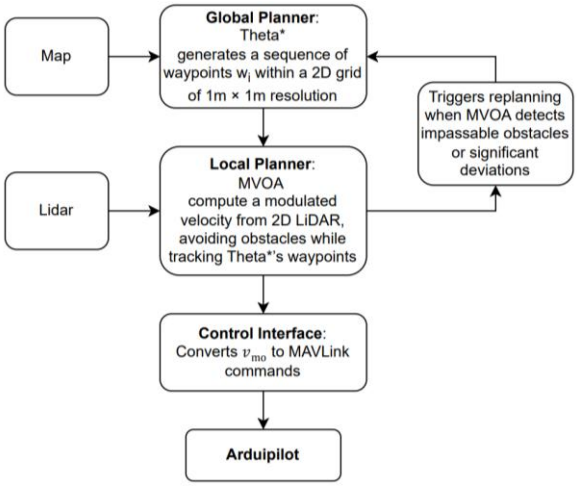

Figure 1. System architecture for autonomous UAV navigation

2.2. Theta* global path planning

Theta* is an enhanced variant of A* that allows any-angle connections via line-of-sight, producing shorter and smoother paths compared to grid-aligned A*. This property makes it well-suited for UAVs by reducing sharp turns and ensuring kinematically feasible trajectories [21], [25]. In our implementation, standard modules (input mapping, heuristic search, line-of-sight checks, and path smoothing [24]) are adapted for UAV navigation, with dynamic replanning triggered when local avoidance blocks progress [27].

The cost function for a node n with parent p and neighbor s is $g(s) = \min\big(g(p) + c(p,s), g(p') + c(p',s)\big)$, where $g(s)$ is the cost to reach s, $c(p,s)$ is the Euclidean distance if line-of-sight exists, and p' is the parent of p. The heuristic $h(s)$ is $h(s) = \left\|\xi_{\text{goal}} - s\right\|$.

The algorithm outputs a sequence of waypoints wp, spaced 1m apart, ensuring the UAV can follow the path with minimal deviation. The nominal velocity v^N toward the next waypoint wp_i is:

$$v^N = v_{\max} \cdot \frac{wp_i - \xi}{\|wp_i - \xi\|}, v_{\max} = 2 \text{ m/s}$$

2.3. Modulated velocity obstacle avoidance

The MVOA algorithm computes a modulated velocity v_{mo} that balances waypoint tracking with obstacle avoidance. To remain lightweight, it treats all LiDAR points as a single obstacle block [19], [20] and estimates obstacle motion via centroid tracking. This enables real-time operation without clustering or complex prediction models.

2.3.1. Algorithm implementation overview

The MVOA algorithm is implemented as a ROS Noetic node that processes LiDAR data and integrates with Theta* waypoints to generate safe velocities. The workflow is: acquire LiDAR scans from /scan; represent all points as a single obstacle block (reference direction, minimum distance); estimate obstacle velocity from centroid motion; compute a modulation matrix to adjust the nominal velocity; integrate with Theta* using adaptive weighting and trigger replanning if blocked; perform safety checks by predicting a 1s trajectory with ≥0.6 m clearance and scale velocity if necessary; finally, publish the safe velocity to /cmd_vel (geometry_msgs/Twist) or convert to MAVLink commands for ArduPilot.

2.3.2. Modulated velocity obstacle avoidance workflow

The MVOA algorithm processes LiDAR data and computes the final velocity through a streamlined pipeline, incorporating obstacle representation, velocity modulation, and safety checks. Below, we describe the entire workflow as a unified process, with detailed explanations of each mathematical formulation to clarify its role in achieving safe and efficient navigation.

Step 1: processing LiDAR data and representing obstacles

MVOA begins by receiving a 2D LiDAR point cloud $\mathcal{P} = \{\xi_i^p = (x_i, y_i) \mid i = 1, \ldots, N^p\}$, where each point ξ_i^p denotes the position of an obstacle relative to the UAV. To reduce complexity, all LiDAR points are aggregated into a single obstacle block, described by four quantities:

a. Unified obstacle block position: $\mathrm{r}(\xi) = \text{mean}\left(\frac{\xi_i^p - \xi}{\|\xi_i^p - \xi\|} \,\middle|\, \xi_i^p \in \mathcal{P}\right)$, where ξ is the UAV position. Each vector $\xi_i^p - \xi$ points from the UAV to a LiDAR return, and the mean provides a representative direction. This approximates the centroid direction of the obstacle block.

b. Distance to obstacle block: $D(\xi) = \min_{\xi_i^p \in \mathcal{P}} \left\|\xi_i^p - \xi\right\| - \left(R + R_{\text{margin}}\right)$, with UAV radius $R = 0.5$ m and safety margin $R_{\text{margin}} = 0.05$ m. This gives a conservative estimate of clearance between the UAV and the closest obstacle.

c. Weight calculation: $w = \left(\frac{1}{D(\xi)}\right)^2$. Closer obstacles yield higher weights, ensuring that imminent threats dominate the avoidance behaviors.

d. Reference direction: $\hat{r}(\xi) = \frac{r(\xi)}{\|r(\xi)\|}$, if $w \leq 100$. If $w > 100$, normalization is enforced to avoid numerical instability. The unit vector $\hat{r}(\xi)$ thus provides a stable avoidance direction toward the obstacle centroid.

Step 2: estimating dynamic obstacle motion

To handle dynamic obstacles, MVOA estimates their velocity $\dot{\xi}_{\text{obs}}$ by tracking the centroid of the obstacle block across two consecutive LiDAR scans separated by Δt=100 ms (10 Hz):

$$\dot{\xi}_{\text{obs}} = \frac{\text{centroid}(\mathcal{P}, t) - \text{centroid}(\mathcal{P}, t - \Delta t)}{\Delta t}$$

here, centroid $(\mathcal{P}, t)$ corresponds to the obstacle position computed in step 1. This method assumes locally constant velocity, suitable for moderately moving objects such as UAVs. If no previous scan exists, $\dot{\xi}_{\text{obs}}$ is set to zero, treating the obstacle as static. This lightweight estimation enables efficient short-term avoidance without requiring complex prediction models.

Step 3: constructing the modulation matrix for static obstacles

For static obstacles ($\dot{\xi}_{\text{obs}} = 0$), MVOA constructs a modulation matrix $M(\xi, v^N)$ to adjust the nominal velocity v^N, steering the UAV away from obstacles while preserving motion in safe directions. The matrix is defined as: $E(\xi) = [\hat{r}(\xi), e_1(\xi)], e_1(\xi) = \frac{(-\widehat{r_y}, \widehat{r_x})}{\sqrt{\widehat{r_x^2} + \widehat{r_y^2}}}$, where $\hat{r}(\xi)$ is the normalized direction to the obstacle, pointing from the UAV to the obstacle centroid, $e_1(\xi)$ is the perpendicular vector, forming an orthogonal basis with $\hat{r}(\xi)$ for velocity modulation.

The eigenvalues λ_r and λ_e control the modulation strength:

$$\lambda_r = \begin{cases} \cos\left(\frac{\pi}{2}\|\hat{r}(\xi)\|\right) \text{ if } \|\hat{r}(\xi)\|<2 \\ -1 \text{ otherwise} \end{cases}, \lambda_e = \begin{cases} 1+\sin\left(\frac{\pi}{2}\|\hat{r}(\xi)\|\right) \text{ if } \|\hat{r}(\xi)\|<1 \\ 2\sin\left(\frac{\pi}{2\|\hat{r}(\xi)\|}\right) \text{ otherwise} \end{cases}$$

Assuming $\|\hat{r}(\xi)\|$ represents the distance $D(\xi)$, λ_r reduces velocity toward the obstacle as $D(\xi)$ decreases below 2m, λ_e amplifies tangential motion to maneuver around the obstacle, especially when $D(\xi) < 1$ m.

The modulation matrix is: $M(\xi, v^N) = E(\xi)\text{diag}(\lambda_r, \lambda_e)E(\xi)^{-1}$. This matrix adjusts the velocity by scaling its radial and tangential components, ensuring the UAV avoids the obstacle while maintaining smooth motion.

Step 4: computing modulation term

The modulation term $\dot{\xi}$ is computed to avoid obstacles while following the nominal velocity v^N. For static obstacles ($\dot{\xi}_{\text{obs}} = 0$): $\dot{\xi} = M(\xi, v^N)v^N$. This adjusts v^N using the modulation matrix $M(\xi, v^N)$, reducing the velocity toward the obstacle while promoting motion around it. For dynamic obstacle: $\dot{\xi} = M(\xi, v^N)\left(v^N - \dot{\xi}_{\text{obs}}\right) + \dot{\xi}_{\text{obs}}$. Here, $v^N - \dot{\xi}_{\text{obs}}$ is the relative velocity, adjusted by $M(\xi, v^N)$ to avoid collision, then converted back to the global frame by adding $\dot{\xi}_{\text{obs}}$. This ensures the UAV steers clear of the obstacle's predicted path.

Step 5: balancing global and local objectives with adaptive weighting

MVOA combines the modulation term $\dot{\xi}$ with the nominal velocity v^N to balance global path tracking and local obstacle avoidance: $v_{\text{mo}} = w_g v^N + w_l \dot{\xi}, w_l = 1 - w_g,\ w_g = \exp\left(-\frac{d_{\min}}{D_{\text{scal}}} \cdot \frac{N_{\text{close}}}{N^p}\right)$, where $d_{\min} = D(\xi)$, N_{close} is number of LiDAR points with $D_i(\xi) < 1m$, D_{scal} is calling factor to adjust the sensitivity of w_g. The weight w_g prioritizes v^N (global path) when obstacles are far ($v^N \rightarrow 1$), and $\dot{\xi}$ (local avoidance) when obstacles are close ($w_g \rightarrow 0$). If $d_{\min} < 0.6\ m$ and no progress is made toward the waypoint for 2 seconds, MVOA triggers Theta* replanning.

Step 6: enforcing safety and dynamic constraints

MVOA ensures safety by predicting the UAV's trajectory over T=1s is $d_{\text{traj}} = \min_{t\in[0,T],i} \left\|\xi_i^p - \xi\right\| - \left(R + R_{\text{margin}}\right)$. If $d_{\text{traj}} < d_{\text{safe}} = 0.6$, scale $v = v_{\text{mo}} \cdot \frac{d_{\text{traj}}}{d_{\text{safe}}}$. Dynamic constrain are also applied: $v = \min(\|v\|, v_{\max})$. These limit the velocity magnitude to $v_{\max}$, ensuring feasible maneuvers.

2.4. Integration of Theta* and modulated velocity obstacle avoidance

The integration of Theta* and MVOA combines global optimality with local reactivity. Theta* generates smooth waypoints, while MVOA ensures real-time avoidance using 2D LiDAR [24], [25]. This is achieved through:

- Waypoint tracking: Theta* outputs waypoints, and MVOA computes velocities v^N. Adaptive weights (w_g, w_l) balance global guidance with local avoidance, keeping the UAV on the global path unless obstacles force deviation.
- Dynamic replanning: if MVOA detects danger (d_{min} <0.6 m and no progress for 2 s), it signals Theta* to replan with updated LiDAR data, improving robustness in dynamic environments.
- Narrow passages: in tight spaces (≈1.5 m wide), MVOA's safety checks prevent collisions while Theta*'s any-angle paths avoid overly conservative routing [27].
- Dynamic obstacles: MVOA estimates obstacle velocity ξ_{obs} and shares it with Theta*, enabling paths that avoid predicted collision zones.

2.5. ArduPilot integration via MAVLink

The framework integrates with ArduPilot via MAVLink to execute MVOA's modulated velocity commands. The 2D velocity $v_{\text{mo}} = \left(v_x, v_y\right)$ is converted into the North-East-Down (NED) frame as $v_{\text{north}} = v_x, v_{\text{east}} = v_y$. These components are encoded into a SET_POSITION_TARGET_LOCAL_NED message with type mask 0b0000111111000111, enabling velocity-only control. The message, transmitted at 10 Hz through a ROS Noetic MAVROS node, is aligned with ArduPilot's local NED system. Upon reception, ArduPilot's internal PID controller translates the velocity inputs into roll, pitch, yaw, and thrust

commands, ensuring that high-level planning and local avoidance are accurately executed in real or simulated flights.

3. RESULTS AND DISCUSSION

The proposed framework integrates Theta* for global planning, MVOA for local avoidance, and ArduPilot control via MAVLink, all implemented on Ubuntu with ROS Noetic. Real-time tests were conducted in a Gazebo 10 m×10 m environment with static and dynamic obstacles.

Theta*, implemented as a C++ ROS node, generates smooth any-angle paths on a 1 m grid using Bresenham's line-of-sight and cubic spline smoothing, with a 0.6 m obstacle buffer. It subscribes to /map and /scan for occupancy and LiDAR data, publishing waypoints to /waypoints. MVOA, running at 10 Hz, processes 360 LiDAR points as a unified obstacle block [19], [20], tracking waypoints via nominal velocities modulated for obstacle proximity. Safety checks maintain 0.6 m clearance, and blocked progress (>2 s) triggers Theta* replanning.

Two experiments compared MVOA-only navigation with the combined Theta*+MVOA approach. Using an Iris quadrotor with LiDAR, both trials aimed to reach a predefined goal. Results in RViz and trajectory plots showed that while MVOA alone achieved obstacle avoidance, the integrated Theta*+MVOA system produced smoother, shorter, and more efficient trajectories, demonstrating the benefits of global–local integration.

In the first experiment, using only MVOA, the UAV successfully avoided all static and dynamic obstacles by computing real-time velocities from LiDAR data. However, without global guidance, it followed reactive, locally optimal trajectories [14], leading to detours, oscillations, and inefficiencies in cluttered areas or narrow passages (≈1.5 m) [6], [27]. The resulting path measured 20.4 m with a completion time of 35.3 s, as shown in Figure 2. The trajectories in Gazebo (Figure 2(a)) and RViz (Figure 2(b)) appear jagged and circuitous, reflecting the limitations of purely local navigation. Figure 3 further illustrates the reactive velocity commands (v_x, v_y) generated by MVOA during flight.

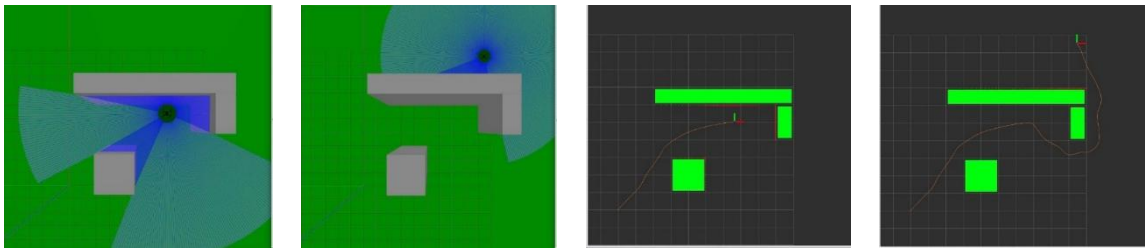

(a) (b)

Figure 2. UAV trajectory using MVOA-only navigation; (a) simulated flights in the Gazebo environment and (b) UAV trajectories visualized in RViz

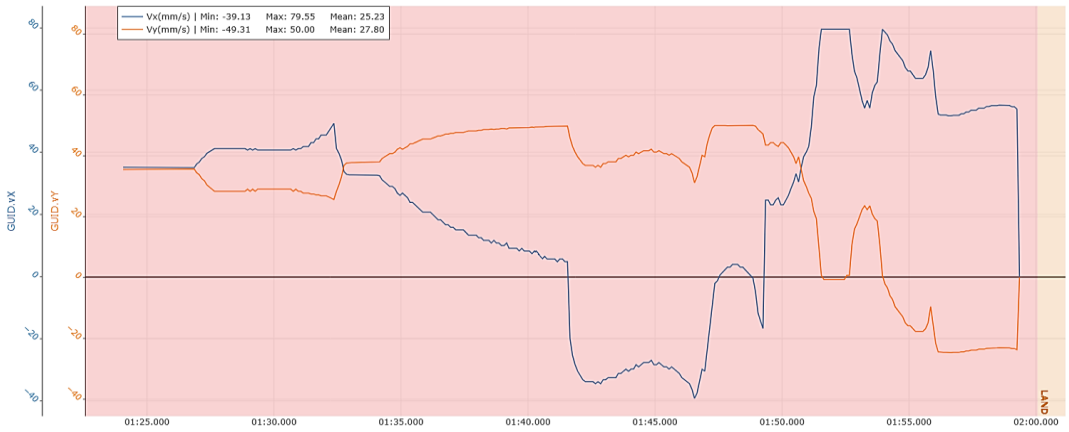

Figure 3. Velocity guide of MVOA-only navigation

The second experiment evaluated the integration of Theta* with MVOA, where Theta* provided optimized waypoints and MVOA computed safe velocities for execution. This combination allowed the UAV to follow a more direct and efficient trajectory, reducing unnecessary detours while ensuring reliable obstacle avoidance.

As a result, the total path length decreased to 14.3 m, and the completion time was shortened to 24.2 s. The resulting trajectory, shown in Figure 4, is notably smoother and closer to the optimal path while respecting safety constraints. Figure 4(a) illustrates the simulated flight in Gazebo, and Figure 4(b) presents the corresponding RViz visualization, both confirming the improved navigation performance. Figure 4(c) further depicts the velocity commands (v_x, v_y) over time, highlighting the coordinated effect of Theta*'s global guidance and MVOA's reactive adjustments.

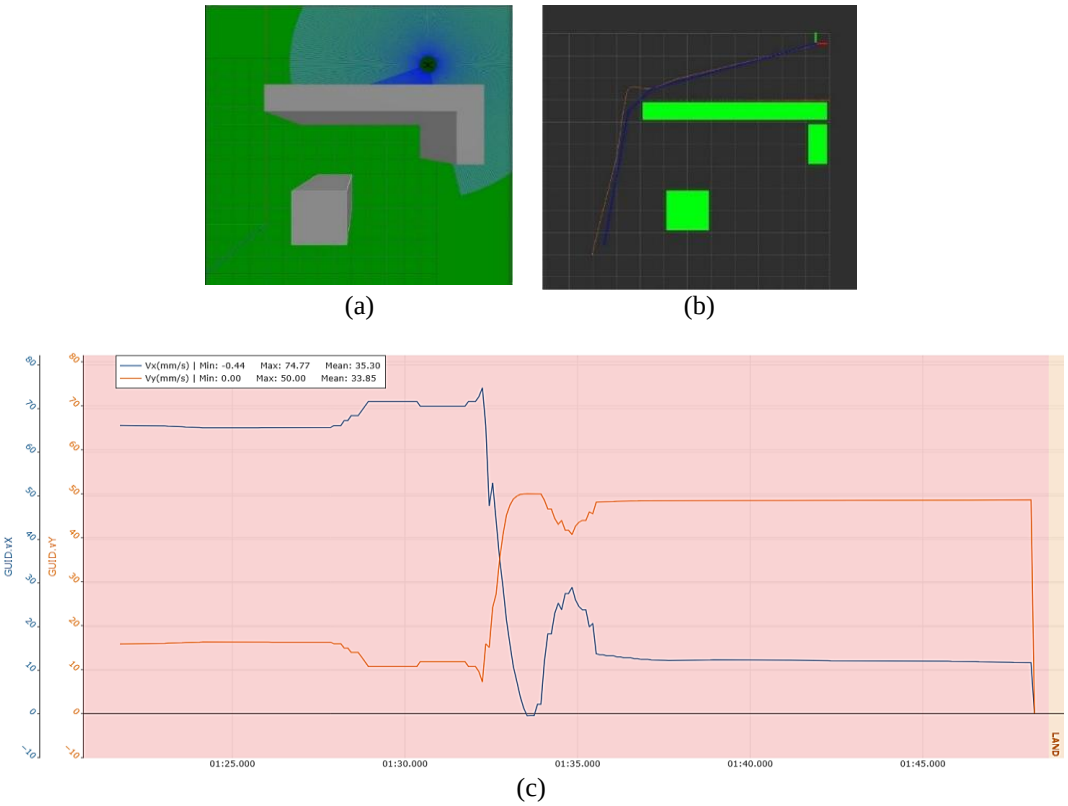

(a) (b)

(c)

Figure 4. UAV trajectory using Theta* and MVOA integrated navigation; (a) UAV operation in the Gazebo environment, (b) UAV trajectories visualized in Rviz, and (c) velocity guide of Theta* and MVOA integrated navigation

To further validate the consistency of both navigation strategies, we conducted five repeated trials for each method under identical conditions. The resulting trajectories are shown in Figure 5, where Figure 5(a) presents the paths generated by MVOA-only navigation, and Figure 5(b) shows the trajectories obtained using the integrated Theta* and MVOA navigation. The overlayed paths demonstrate the repeatability of the experiments. In all cases, Theta*+MVOA provided shorter and smoother paths than MVOA-Only. Quantitative results are summarized in Table 1. For MVOA-only navigation, the average path length was 20.4 m (±0.2 m) with a mean completion time of 35.3 s (±0.7 s), confirming the inefficiencies observed in the trajectories. By comparison, the Theta*+MVOA integration reduced the average path length to 14.4 m (±0.3 m) and the mean completion time to 24.6 s (±1.2 s). These results demonstrate not only significant improvements in efficiency but also high repeatability, as indicated by the small standard deviations across runs.

The superior performance of the combined Theta* and MVOA framework stems from their complementary strengths. Theta* provides a global perspective, using line-of-sight checks and cubic spline interpolation to produce efficient, UAV-friendly paths. MVOA enhances this by handling local dynamics, such as sudden obstacle movements, with rapid velocity modulation and safety checks. The integration, facilitated by ROS Noetic and MAVLink, ensures seamless communication between planning and control, as

evidenced by the consistent 10 Hz command rate to the Arduipilot. The results also validate the system's robustness across diverse scenarios, including narrow passages and dynamic obstacle interactions, making it suitable for applications like swarm UAV coordination and terrain surveying.

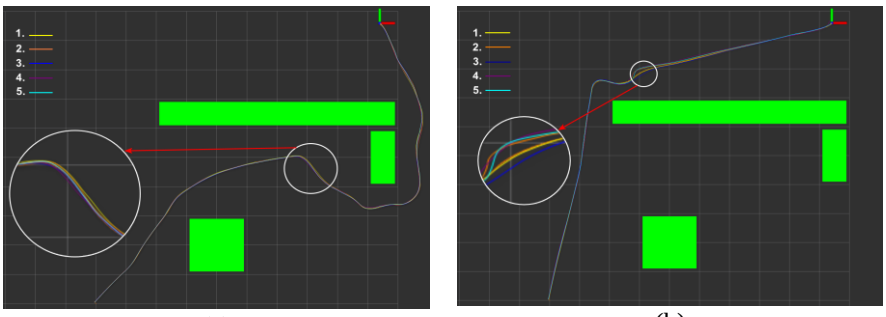

(a) (b)

Figure 5. Comparison of UAV trajectories; (a) MVOA-only navigation and (b) Theta* and MVOA integrated navigation

Table 1. Experimental results over 5 runs for each method

Method	Run 1: path length (m)	Run 1: time (s)	Run 2: path length (m)	Run 2: time (s)	Run 3: path length (m)	Run 3: time (s)	Run 4: path length (m)	Run 4: time (s)	Run 5: path length (m)	Run 5: time (s)	Mean path (m)±Std	Mean time (s)±Std
MVOA-only	20.1	34.2	20.5	35.8	20.6	35.6	20.2	34.8	20.5	35.9	20.4±0.2	35.3±0.7
Theta+MVOA*	14.1	23.6	14.5	24.5	14.3	23.4	14.6	25.4	14.7	26.1	14.4±0.3	24.6±1.2

4. CONCLUSION

This study presented a hybrid framework for autonomous UAV navigation that integrates Theta* for global path planning with a simplified MVOA for local obstacle avoidance. Simulation results in a 10 m×10 m Gazebo environment with static and dynamic obstacles demonstrated that the framework maintained a 0.6 m safety margin at 10 Hz and significantly outperformed MVOA-only navigation, reducing path length from 20.4 m to 14.3 m and mission time from 35.3 s to 24.2 s. Velocity analysis further showed smoother and more stable trajectories, confirming both computational efficiency and operational benefits.

While effective, the current work is limited to 2D navigation in simulation. The single-obstacle-block assumption of MVOA, although lightweight, may struggle in highly cluttered environments. Moreover, hardware validation was not included, as the focus was on controlled simulation experiments. Future work will address these gaps by extending the framework to 3D navigation with stereo LiDAR or RGB-D sensing, performing robustness testing under sensor noise and dynamic disturbances, and validating performance on real UAV platforms with proper sensor calibration and communication constraints.

Taken together, the findings establish the proposed framework as both efficient and practical, providing shorter, faster, and smoother trajectories while ensuring safety. These contributions lay a strong foundation for diverse UAV applications, including terrain surveying, indoor navigation, and swarm coordination, and pave the way for scalable real-world deployment in more complex 3D environments.

ACKNOWLEDGMENTS

The authors would like to thank Duy Tan University (DTU), Vietnam for the support.

FUNDING INFORMATION

Authors state no funding involved.

AUTHOR CONTRIBUTIONS STATEMENT

This journal uses the Contributor Roles Taxonomy (CRediT) to recognize individual author contributions, reduce authorship disputes, and facilitate collaboration.

Name of Author	C	M	So	Va	Fo	I	R	D	O	E	Vi	Su	P	Fu
Hoang Thuan Tran		✓		✓			✓			✓		✓		✓
Dong LT. Tran		✓		✓		✓	✓			✓			✓	
Chi Thanh Vo	✓	✓	✓	✓	✓	✓		✓	✓	✓	✓		✓	

C : **C**onceptualization
M : **M**ethodology
So : **So**ftware
Va : **Va**lidation
Fo : **Fo**rmal analysis
I : **I**nvestigation
R : **R**esources
D : **D**ata Curation
O : Writing - **O**riginal Draft
E : Writing - Review & **E**diting
Vi : **Vi**sualization
Su : **Su**pervision
P : **P**roject administration
Fu : **Fu**nding acquisition

CONFLICT OF INTEREST STATEMENT

The authors declare that they have no known competing financial interests or personal relationships that could have appeared to influence the work reported in this paper.

DATA AVAILABILITY

The data supporting the findings of this study are available from the corresponding author, Chi Thanh Vo, upon reasonable request. Public disclosure is restricted to protect research privacy and security. However, the author is willing to share the relevant data for justified academic or research purposes.

REFERENCES

[1] S. Manfreda *et al.*, "On the use of unmanned aerial systems for environmental monitoring," *Remote Sensing*, vol. 10, no. 4, pp. 1–28, Apr. 2018, doi: 10.3390/rs10040641.

[2] F. Toscano *et al.*, "Unmanned Aerial Vehicle for Precision Agriculture: A Review," *IEEE Access*, vol. 12, pp. 69188–69205, 2024, doi: 10.1109/ACCESS.2024.3401018.

[3] M. Erdelj, M. Król, and E. Natalizio, "Wireless Sensor Networks and Multi-UAV systems for natural disaster management," *Computer Networks*, vol. 124, pp. 72–86, Sep. 2017, doi: 10.1016/j.comnet.2017.05.021.

[4] D. L. T. Tran, T. C. Vo, H. T. Tran, M. T. Nguyen, and H. T. Do, "Design Optimal Backstepping Controller for Quadrotor Based on Lyapunov Theory for Disturbances Environments," *arXiv preprint*, pp. 3–7, 2024, doi: 10.48550/arXiv.2503.06824.

[5] J. Kumar, Himanshu, H. Kandath, and P. Agrawal, "Vision based UAV Navigation through Narrow Passages," *arXiv preprint*, 2023, doi: 10.48550/arXiv.2303.15803.

[6] D. N. Bui, T. H. Khuat, M. D. Phung, T. H. Tran, and D. L. T. Tran, "Model Predictive Control for Optimal Motion Planning of Unmanned Aerial Vehicles," in *2024 International Conference on Control, Robotics and Informatics (ICCRI)*, Danang, Vietnam: IEEE, Jul. 2024, pp. 103–108, doi: 10.1109/ICCRI64298.2024.00025.

[7] J. Tordesillas and J. P. How, "PANTHER: Perception-Aware Trajectory Planner in Dynamic Environments," *IEEE Access*, vol. 10, pp. 22662–22677, 2022, doi: 10.1109/ACCESS.2022.3154037.

[8] D. Palossi, F. Conti, and L. Benini, "An open source and open hardware deep learning-powered visual navigation engine for autonomous nano-UAVs," in *2019 15th International Conference on Distributed Computing in Sensor Systems (DCOSS)*, Santorini, Greece: IEEE, May. 2019, pp. 604–611, doi: 10.1109/DCOSS.2019.00111.

[9] B. Lindqvist, S. S. Mansouri, J. Haluška, and G. Nikolakopoulos, "Reactive Navigation of an Unmanned Aerial Vehicle with Perception-Based Obstacle Avoidance Constraints," *IEEE Transactions on Control Systems Technology*, vol. 30, no. 5, pp. 1847–1862, Sep. 2022, doi: 10.1109/TCST.2021.3124820.

[10] F. Ahmed, J. C. Mohanta, A. Keshari, and P. S. Yadav, "Recent Advances in Unmanned Aerial Vehicles: A Review," *Arabian Journal for Science and Engineering*, vol. 47, no. 7, pp. 7963–7984, Jul. 2022, doi: 10.1007/s13369-022-06738-0.

[11] D. T. Tran, V. Q. Nguyen, C. V. Nguyen, D. L. T. Tran, H. T. Tran, and N. D. Anh, "Improved Accuracy of Path System on Creating Intelligence Base," in *International Conference on Advances in Information and Communication Technology*, Cham: Springer Nature Switzerland, 2023, pp. 194–205, doi: 10.1007/978-3-031-49529-8_21.

[12] D. Fox, W. Burgard, and S. Thrun, "The dynamic window approach to collision avoidance," *IEEE Robotics and Automation Magazine*, vol. 4, no. 1, pp. 23–33, Mar. 1997, doi: 10.1109/100.580977.

[13] Y. Cao and N. M. Nor, "An improved dynamic window approach algorithm for dynamic obstacle avoidance in mobile robot formation," *Decision Analytics Journal*, vol. 11, pp. 1–14, Jun. 2024, doi: 10.1016/j.dajour.2024.100471.

[14] J. Borenstein and Y. Koren, "The Vector Field Histogram—Fast Obstacle Avoidance for Mobile Robots," *IEEE Transactions on Robotics and Automation*, vol. 7, no. 3, pp. 278–288, Jun. 1991, doi: 10.1109/70.88137.

[15] H. Rashed *et al.*, "Generalized object detection on fisheye cameras for autonomous driving: Dataset, representations and baseline," *Proceedings of the IEEE/CVF Winter Conference on Applications of Computer Vision*, 2021, pp. 2272–2280, doi: 10.1109/WACV48630.2021.00232.

[16] P. E. Hart, N. J. Nilsson, and B. Raphael, "A Formal Basis for the Heuristic Determination of Minimum Cost Paths," *IEEE Transactions on Systems Science and Cybernetics*, vol. 4, no. 2, pp. 100–107, 1968, doi: 10.1109/TSSC.1968.300136.

[17] K. Daniel, A. Nash, S. Koenig, and A. Felner, "Theta*: Any-angle path planning on grids," *Journal of Artificial Intelligence Research*, vol. 39, pp. 533–579, Oct. 2010, doi: 10.1613/jair.2994.

[18] D. Harabor and A. Grastien, "An optimal any-angle pathfinding algorithm," *Proceedings of the International Conference on Automated Planning and Scheduling*, vol. 23, pp. 308–311, Jun. 2013, doi: 10.1609/icaps.v23i1.13609.

[19] P. Fiorini and Z. Shiller, "Motion planning in dynamic environments using velocity obstacles," *International Journal of Robotics Research*, vol. 17, no. 7, pp. 760–772, Jul. 1998, doi: 10.1177/027836499801700706.

[20] W. Xia, F. Song, and Z. Peng, "Dynamic Obstacle Perception Technology for UAVs Based on LiDAR," *Drones*, vol. 9, no. 8, pp.

1–15, Jul. 2025, doi: 10.3390/drones9080540.
[21] S. Primatesta, G. Guglieri, and A. Rizzo, "A Risk-Aware Path Planning Strategy for UAVs in Urban Environments," *Journal of Intelligent and Robotic Systems: Theory and Applications*, vol. 95, no. 2, pp. 629–643, Aug. 2019, doi: 10.1007/s10846-018-0924-3.
[22] J. Liu, W. Luo, G. Zhang, and R. Li, "Unmanned Aerial Vehicle Path Planning in Complex Dynamic Environments Based on Deep Reinforcement Learning," *Machines*, vol. 13, no. 2, pp. 1–26, Feb. 2025, doi: 10.3390/machines13020162.
[23] Z. Xu, H. Shen, X. Han, H. Jin, K. Ye, and K. Shimada, "LV-DOT: LiDAR-visual dynamic obstacle detection and tracking for autonomous robot navigation," *arXiv preprint*, 2025, doi: 10.48550/arXiv.2502.20607.
[24] Y. Zhou, L. Yan, Y. Han, H. Xie, and Y. Zhao, "A Survey on the Key Technologies of UAV Motion Planning," *Drones*, vol. 9, no. 3, pp. 1–37, Mar. 2025, doi: 10.3390/drones9030194.
[25] F. Gao, L. Wang, B. Zhou, X. Zhou, J. Pan, and S. Shen, "Teach-repeat-replan: A complete and robust system for aggressive flight in complex environments," *IEEE Transactions on Robotics*, vol. 36, no. 5, pp. 1526–1545, 2020, doi: 10.1109/TRO.2020.2993215.
[26] Z. Xu, X. Zhan, Y. Xiu, C. Suzuki, and K. Shimada, "Onboard Dynamic-Object Detection and Tracking for Autonomous Robot Navigation With RGB-D Camera," *IEEE Robotics and Automation Letters*, vol. 9, no. 1, pp. 651–658, Jan. 2024, doi: 10.1109/LRA.2023.3334683.
[27] Z. Huang, C. Jiang, C. Shen, B. Liu, T. Huang, and M. Zhang, "A Hybrid Dynamic Path-Planning Method for Obstacle Avoidance in Unmanned Aerial Vehicle-Based Power Inspection," *World Electric Vehicle Journal*, vol. 16, no. 1, p. 22, Jan. 2025, doi: 10.3390/wevj16010022.
[28] Z. Xu, X. Zhan, B. Chen, Y. Xiu, C. Yang, and K. Shimada, "A real-time dynamic obstacle tracking and mapping system for UAV navigation and collision avoidance with an RGB-D camera," in *2023 IEEE International Conference on Robotics and Automation (ICRA)*, London, United Kingdom, IEEE, May. 2023, pp. 10645–10651, doi: 10.1109/ICRA48891.2023.10161194.
[29] L. Zhang, Y. Hu, Y. Deng, F. Yu, and D. Zou, "Mapless Collision-Free Flight via MPC using Dual KD-Trees in Cluttered Environments," *arXiv preprint*, 2025, doi: 10.48550/arXiv.2503.10141.
[30] J. Li, X. Xu, Z. Liu, S. Yuan, M. Cao, and L. Xie, "AEOS: Active Environment-aware Optimal Scanning Control for UAV LiDAR-Inertial Odometry in Complex Scenes," *arXiv preprint*, 2025, doi: 10.48550/arXiv.2509.09141.
[31] Z. Jian *et al.*, "Dynamic Control Barrier Function-based Model Predictive Control to Safety-Critical Obstacle-Avoidance of Mobile Robot," *arXiv preprint*, 2022, doi: 10.48550/arXiv.2209.08539.

BIOGRAPHIES OF AUTHORS

Hoang Thuan Tran earned a B.E. in System Measurement and Control from Danang University of Science and Technology (1998), an M.S. in Network and Electrical Systems from the University of Danang (2009), and a Ph.D. in Electronics and Communication Technology from the University of Technology - VNU, Hanoi (2016). His research focuses on data sensors, wireless networks, and control automation. He is currently the Dean of the Institute of Aerospace Technology and Engineering at Duy Tan University, Da Nang. He can be contacted at email: tranthuanhoang@duytan.edu.vn.

Dong LT. Tran received the B.S. degree from the Duy Tan University, Da Nang, Vietnam, in 2009, the M.S. degree from the Duy Tan University, Da Nang, Vietnam, in 2012, and became a Ph.D. student at Thai Nguyen University from 2022 to the present. He is currently the Vice Dean of the Institute of Aerospace Technology and Engineering at Duy Tan University, Da Nang and the Lecture of the Faculty of Electronic Engineering, Duy Tan University, Da Nang, Vietnam. His main research interests are object-oriented system design, embedded systems, drones, and mobile robots. He can be contacted at email: tranthangdong@duytan.edu.vn.

Chi Thanh Vo received a degree in Mechatronic Engineering from Danang University of Technology, Vietnam in 2013. He is currently an expert at Center for Electrical and Electronic Engineering, Duy Tan University, Vietnam (CEE). He has interest and expertise in research topics in the field of embedded programming, automatic control, drones, and mobile robots. He can be contacted at email: vochithanh1@dtu.edu.vn.